RESEARCH | Article in Press

Effects of ultrasound pre-treatment on the physicochemical, structural, thermal, and functional properties of cacauí (*Theobroma speciosum* Willd. ex Spreng.)

Josiana Moreira Mar · Daniel de Queiroz Rocha · Adriano de Souza Carolino · Camila Macena Ruzo · Daniel Nascimento Motta · Florência João Macamo · Erickson Oliveira dos Santos · Francisca das Chagas do Amaral Souza · Valdely Ferreira Kinupp · Renilto Frota Correa · Edgar Aparecido Sanches · Pedro Henrique Campelo · Jaqueline de Araújo Bezerra

Received: 13 April 2026 / Accepted: 14 August 2026
© The Author(s) 2026

Abstract

Theobroma speciosum Willd. ex Spreng (cacauí) is a native Amazonian species whose seeds remain underutilized despite their nutritional and bioactive potential. This study evaluated the effects of ultrasound pre-treatment on the physicochemical, structural, thermal, and functional properties of cacauí seed powder, focusing on the release of bioactive compounds. Ultrasound pre-treatments were applied at different amplitudes (20, 40, and 70% of probe amplitude) and processing times (4, 8, and 12 min), while the ultrasound frequency was kept constant throughout the experiments. Analyses included proximate composition, Fourier-transform infrared spectroscopy (FTIR), scanning electron microscopy (SEM), thermogravimetric analysis (TGA), antioxidant capacity (DPPH, ABTS, and FRAP), total phenolic content (TPC), LC–ESI–QTOF-MS qualitative analysis, and mineral composition. The seed powder exhibited low moisture (2.31–3.98%), high lipid (25.94–28.92%) and carbohydrate (50.31–54.37%) contents, and moderate protein (14.69–16.25%) and ash (1.78–2.85%) levels. FTIR showed that ultrasound modified intermolecular interactions without affecting the chemical integrity of the matrix, whereas SEM revealed increased surface roughness, porosity, and particle fragmentation. LC–ESI–QTOF-MS identified theacrine, highlighting the nutraceutical potential of cacauí. Thermogravimetric analysis indicated only minor changes in thermal stability after treatment. Among the evaluated conditions, the treatment combining 70% amplitude and 12 min of processing (C70/12) produced the highest bioactive compound release, with a 7.5-fold higher TPC, 87.7% higher DPPH, 89.5% higher ABTS, and 51.5% higher FRAP compared to the untreated sample. The mineral profile was dominated by K, P, Mg, and Ca, together with Fe, Zn, Mn, and Cu. These findings demonstrate that ultrasound is an effective and environmentally friendly pre-treatment for enhancing the functional properties and bioactive compound availability of cacauí seed powder, supporting its application as a functional ingredient in food and nutraceutical products.

This Article in Press is shared early to give you faster access to new research. It is citable and carries a permanent DOI. The final edited version will replace it automatically.



https://doi.org/10.1007/s44187-026-01225-z

Published online: 07 November 2026

Discover

Keywords *Theobroma speciosum* Willd. ex Spreng · Ultrasound pre-treatment · Bioactive compounds · Antioxidant activity

1 Introduction

Species of the genus *Theobroma* have attracted increasing scientific interest due to their nutritional value and potential as sources of bioactive compounds with relevant functional and technological properties [22]. Among these species, *Theobroma speciosum* Willd. ex Spreng. (cacauí) has gained attention because of the presence of bioactive metabolites, particularly phenolic compounds, which have been associated with antioxidant capacity and potential applications in functional food development. Phenolic compounds are widely studied due to their ability to interact with reactive oxygen species and contribute to the antioxidant properties of plant-derived ingredients; however, their biological effects depend on factors such as chemical structure, concentration, and bioavailability [24].

The valorization of underexplored Amazonian species has increased interest in developing processing strategies capable of improving the recovery and accessibility of bioactive compounds from plant matrices. Among these technologies, ultrasound-assisted processing has emerged as an environmentally friendly approach due to its ability to enhance mass transfer, reduce processing time, and potentially improve the release of intracellular compounds while limiting the degradation of thermosensitive molecules. In food applications, ultrasound technology may be applied as a pre-treatment step before subsequent processing operations, aiming to modify the plant matrix structure and facilitate the extraction or availability of target compounds.

Ultrasound pre-treatment refers to the application of ultrasonic energy to a raw material before the main processing stage. In the present study, ultrasound was applied to cacauí seeds prior to powder production to promote structural modifications in the matrix and improve the accessibility of chemical constituents. The effects of ultrasound depend on the operational parameters applied, including frequency, power, treatment time, and the type of ultrasonic system. The technology used in this study operates through acoustic cavitation, a phenomenon characterized by the formation, growth, and collapse of microbubbles in the medium. This phenomenon generates localized shear forces, microjets, and mechanical effects that may disrupt cellular structures, increase permeability, and enhance mass transfer between the matrix and surrounding médium [46].

Previous studies have demonstrated that ultrasound-assisted technologies can increase the extraction efficiency of phenolic compounds, flavonoids, and other secondary metabolites from different plant matrices. The mechanical effects associated with acoustic cavitation may induce changes in plant tissue organization, including increased porosity, disruption of cell walls, and improved accessibility of intracellular compounds. These modifications can contribute to higher recovery of bioactive compounds and enhanced antioxidant potential of plant-derived ingredients [13]. Nevertheless, the effectiveness of ultrasound treatment is highly dependent on the characteristics of the raw material and the applied processing conditions.

Although *T. speciosum* represents a promising Amazonian resource, information regarding the physicochemical composition, structural characteristics, functional properties, and potential food applications of its seeds remains limited compared with other *Theobroma* species, particularly when emerging technologies are applied. Recent studies on the use and valorization of *Theobroma* species have highlighted the potential of cocoa-related seeds as sources of bioactive compounds and functional ingredients for food applications, reinforcing the need for further investigation of underutilized species.

Recent advances in ultrasound-assisted processing have reinforced the potential of this technology as a sustainable and efficient approach for enhancing the recovery, preservation, and bioavailability of bioactive compounds in plant-derived materials [42]. The cavitation phenomenon promoted by ultrasound improves mass transfer through cell wall disruption, resulting in higher extraction yields of phenolic compounds, flavonoids, minerals, and other functional constituents while minimizing thermal degradation [2]. In addition, ultrasound has

demonstrated the ability to preserve physicochemical quality, antioxidant activity, and sensory attributes in different food matrices, supporting its application as a green technology for the development of functional ingredients and value-added products [2]. Furthermore, recent studies have shown that ultrasound processing can enhance the bioaccessibility and functional performance of bioactive compounds while providing optimized, data-driven processing strategies for food applications ([19] p. 2). These findings highlight the relevance of investigating ultrasound-assisted processing in Amazonian species with limited scientific information, such as *Theobroma speciosum*, to expand their technological and industrial applications.

Therefore, this study aimed to evaluate the effect of ultrasound pre-treatment on the chemical composition, antioxidant activity, microstructural characteristics, and thermal properties of cacauí (*Theobroma speciosum*) seed powder. By combining physicochemical and functional analyses, this work provides new insights into the potential application of ultrasound-assisted processing for the valorization of an Amazonian *Theobroma* species and its use as a source of bioactive-rich ingredients for food and related industries.

2 Materials and methods

2.1 Sample preparation

Cacauí seed powder was obtained at km 14 in the municipality of Careiro Castanho, Amazonas, Brazil, under SisGen registration nº. A9F3E4F, and subsequently subjected to a roasting process at 125 °C for 30 min. For the ultrasonic treatment, a sample-to-water ratio of 1:10 (w/v) was used. This ratio was selected based on previous studies and preliminary trials, as it provides sufficient solvent availability to promote efficient acoustic cavitation and homogeneous ultrasound propagation throughout the sample. Ultrasound treatments were performed using power amplitudes of 20, 40, and 70%, corresponding to low, intermediate, and high acoustic energy input levels, which were selected to evaluate the influence of increasing ultrasonic intensity on the physicochemical characteristics and bioactive compounds of cacauí seed powder while minimizing excessive degradation of thermolabile constituents. Treatment times of 4, 8, and 12 min were chosen to investigate the effect of increasing ultrasound exposure on cell disruption and the release of intracellular compounds.

The process was carried out in an ice bath to minimize temperature increases caused by acoustic cavitation and to ensure that the observed effects were primarily associated with the mechanical action of ultrasound rather than thermal effects. During ultrasonic homogenization, the systems were treated using a 25 mm diameter probe operating at a frequency of 20 kHz and nominal power of 750 W (VibraCell VCX 750, Sonics, Shawnee, OK, USA). After the ultrasound (US) process, excess water was removed with paper towel, and the samples were subsequently freeze-dried [37].

2.2 Antioxidant capacity assessment

The free radical scavenging capacity of the samples was evaluated using the DPPH• and ABTS•$^{+}$ assays, as well as the ferric reducing antioxidant power (FRAP) method [21]. After ultrasound treatment at a 1:10 (w/v) ratio, specific aliquots were collected for the antioxidant activity assays.

The free radical scavenging capacity of the samples was evaluated using the DPPH• and ABTS•$^{+}$ assays, as well as the ferric reducing antioxidant power (FRAP) method [21].

For the DPPH• assay, a 100 µM methanolic DPPH• solution was prepared. The extracts (1 mg/mL) were used for the analysis, and 100 µL of the sample extract was added to 1900 µL of the DPPH• solution. Trolox (100–2000 µM) was used as the standard for the calibration curve. The reaction mixture was kept protected from light at room temperature for 30 min, and absorbance was measured at 515 nm using a microplate reader (Epoch 2, BioTek, Winooski, VT, USA). All analyses were performed in triplicate.

The ABTS•+ radical scavenging activity was determined by measuring the reduction in absorbance of the ABTS•+ solution in the presence of antioxidant compounds. The reaction was carried out using a sample-to-radical ratio of 1:10, with a reaction time of 6 min. Absorbance was measured at 750 nm using a microplate reader. The calibration curve was obtained using Trolox as the standard, and the results were expressed as µM Trolox equivalents per mL.

The ferric reducing antioxidant power (FRAP) assay was used to evaluate the ability of the extracts to reduce Fe^{3+} to Fe^{2+} in the presence of the ferric–tripyridyltriazine complex. After incubation of the sample extract with the FRAP reagent at 37 °C for 30 min, absorbance was measured at 593 nm using a UV spectrophotometer. The standard curve was constructed using $FeSO_4$, and the results were expressed as micromolar equivalents of Fe(II) (µM Fe(II)/mL).

2.3 Determination of total phenolic content of extracts (TPC)

Total phenolic content (TPC) was determined using the Folin–Ciocalteu colorimetric method. Initially, the samples were mixed with the Folin–Ciocalteu reagent and allowed to react for 5 min. Subsequently, a 6% sodium bicarbonate solution was added, and the reaction mixture was incubated at room temperature for 90 min. The absorbance was measured at 750 nm using a microplate reader. The results were expressed as milligrams of gallic acid equivalents per milliliter of sample (mg GAE/mL) [23].

2.4 LC–ESI–QTOF-MS qualitative analysis

Chromatographic separation was performed using an ultra-high-performance liquid chromatography (UHPLC) system (ACQUITY UPLC®, Waters Corp., Milford, MA, USA) equipped with a binary solvent manager and an autosampler. An ACQUITY UPLC® BEH C18 column (1.7 µm particle size) was employed and maintained at 40 °C. The autosampler temperature was set at 15 °C, and the injection volume was 10 µL.

The mobile phase consisted of (A) ultrapure water with 0.1% formic acid and (B) methanol containing 0.1% formic acid. The flow rate was set at 0.25 mL min^{-1}. The gradient elution program was as follows: 0–15 min, 2–20% B; 15–20 min, 20–40% B; 20–25 min, 40–80% B; 25–27 min, 80–95% B; held at 95% B until 28 min; followed by re-equilibration to initial conditions (2% B) from 28.5 to 30 min. The total run time was 30 min.

Mass spectrometric detection was carried out using a quadrupole time-of-flight mass spectrometer (QTOF-MS) (Xevo G2-XS QTof, Waters Corp.) equipped with an electrospray ionization (ESI) source operating in positive ion mode (ESI+). The instrument was operated in resolution mode with a mass resolving power of approximately 30,000. Data were acquired over an m/z range of 100–1200 Da in continuum mode.

The ion source parameters were set as follows: capillary voltage, 3.0 kV; sampling cone voltage, 40 V; source temperature, 150 °C; desolvation temperature, 500 °C; cone gas flow, 50 L h^{-1}; and desolvation gas flow, 800 L h^{-1}. The collision energy was applied using a data-independent acquisition (MSE) approach, with low-energy scans at 6 eV and high-energy ramp from 20 to 35 eV to generate fragment ions. Leucine enkephalin was used as the lock-mass reference ($[M+H]^+$ = m/z 556.2771), infused at 10 µL min^{-1}, with acquisition every 15 s to ensure mass accuracy during the analysis. The system was calibrated using a sodium formate solution over the mass range of m/z 92–1174 prior to analysis. Data acquisition and processing were performed using MassLynx™ software (version 4.2, Waters Corp.). Peak detection, deconvolution, and spectral interpretation were conducted using centroided data with automated isotope and charge state recognition.

2.5 High-performance liquid chromatography with diode array detector (HPLC-DAD) for quantitative analysis

A reverse-phase HPLC system (Shimadzu Corporation, Kyoto, Japan) was employed for the quantification of theacrine [4]. The chromatographic system consisted of an autosampler (SIL-20 A), solvent delivery pumps

(LC-20CE), an online degasser (DGU-20A5), a system controller (CBM-20 A), a column oven (CTO-20 A), and a diode-array detector (SPD-M20A), all controlled by LCsolution software (version 1.25 SP5).

Chromatographic separation was performed using an CORTECS T3 column (4.6 × 100 mm, 2.7 µm particle size; Waters Corporation, Milford, MA, USA). The flow rate was set at 1.0 mL/min, and the injection volume was 10 µL. The mobile phase consisted of 0.1% (v/v) aqueous formic acid (solvent A) and methanol (solvent B). Both samples and mobile phase were filtered through a 0.22 µm polyvinylidene difluoride (PVDF) membrane filter (47 mm diameter; Millipore, USA) and degassed in an ultrasonic bath prior to analysis. The gradient elution program was as follows: 10–60% B over 15 min, 60–80% B at 20 min, 80–100% B at 28 min, followed by re-equilibration to 10% B at 30 min. The column temperature was maintained at 35 °C.

The wavelengths for detections were used for confirmation of chromatography peaks and quantification of their corresponding phenolic compounds achieved by comparing their retention time with those of reference standards and by DAD spectra (200–600 nm).

Theacrine standard solutions were prepared in ultrapure water. A stock solution (171.50 mg/L) was prepared from certified reference material and used to obtain working standard solutions by serial dilution, freshly prepared on a daily basis. Calibration was performed at 290 nm over the concentration range of 2.3–45.7 mg/L. The method exhibited excellent linearity, with a coefficient of determination (R^2) of 0.9989 and the regression equation $y = 25036x - 9517.4$. The limit of quantification (LOQ) was determined to be 0.22 mg/L, and the method demonstrated acceptable homoscedasticity across the evaluated concentration range. Method precision showed excellent repeatability, with RSD values ranging from 0.10% to 0.42% (mean RSD = 0.20%). Accuracy, evaluated by recovery assays at three fortification levels, ranged from 95.15% to 103.83%. These results confirm the reliability of the HPLC-DAD method for the quantitative determination of theacrine.

2.6 Proximate composition

The proximate composition of cacauí seed powders was determined according to standardized analytical procedures. Moisture content was measured by oven drying at 105 °C until constant weight, while ash content was obtained by incineration at 550 °C. Lipids were extracted using a Soxhlet apparatus with hexane for 8 h, and protein content was determined by the classical Kjeldahl method (Lutz, 2008). Carbohydrates were quantified by difference, following the methodology described by Ogunlaja et al. [26]. The total energy value was estimated using the equation proposed by Palmeira et al. [30]:

$$\text{Energy (kcal)} = 4 \times (\text{g protein} + \text{g carbohydrates}) + 9 \times (\text{g lipids}).$$

2.7 Fourier transform-infrared (FT-IR) spectroscopy

The chemical profile of the samples was determined using a FTIR−ATR spectrophotometer (Agilent Cary 630) with attenuated total reflection module (FTIR-ATR) from 680 to 4000 cm^{-1}.

2.8 Scanning electron microscopy (SEM)

The Cacauí powders were characterized by Scanning Electron Microscopy (SEM) using a JSM-IT500HR electron microscope (JEOL, Tokyo, Japan), with a 30 kV electron beam and a magnification of 100×.

2.9 Thermogravimetric analysis

The analysis was performed on a thermogravimetric analyzer (DTGA60 H, Shimadzu, Kyoto, Japan), operated under an inert nitrogen atmosphere at a flow rate of 20 mL/minute. In the analysis, 7.0 ± 1 mg of each sample were placed in an alumina crucible and heated to 900 °C, with a heating rate of 10 °C/minute.

2.10 Determination of macro- and microminerals by inductively cacauí seed powder optical emission spectroscopy (ICP-OES)

Acid digestion of 0.3 g of lyophilized sample was carried out using a microwave system MARS 6 (CEM Corporation, EUA) with 10 mL of ultrapure nitric acid (HNO_3). The digestion program consisted of a temperature ramp to 180 °C within 15 min, followed by a holding time of 15 min and subsequent cooling to 70 °C. After digestion, samples were quantitatively diluted to 25 mL with ultrapure water and stored at 4 °C until analysis. Elemental quantification of macro- and microminerals was performed by inductively coupled plasma optical emission spectrometry (ICP-OES) using an Agilent 5800 system (Agilent Technologies), with argon as the nebulizer gas. Calibration curves were constructed using certified reference materials and exhibited excellent linearity ($R^2 > 0.999$), with relative standard errors (%RSE) below 10%, confirming the accuracy, sensitivity, and robustness of the analytical method [21]. Limits of quantification (LOQ) were established based on calibration curves for each analyte. For macrominerals, LOQ values were: K (766.491 nm, 0.5046 mg/L), Mg (279.553 nm, 1.012 mg/L), Ca (396.847 nm, 0.5072 mg/L), and P (213.618 nm, 0.0103 mg/L). For microminerals, LOQ values were: Ba (455.403 nm, 0.1034 mg/L), Cu (327.395 nm, 0.0052 mg/L), Fe (238.204 nm, 0.1027 mg/L), Mn (257.610 nm, 0.0824 mg/L), Ni (231.604 nm, 0.0104 mg/L), and Zn (213.857 nm, 0.0105 mg/L), demonstrating high analytical sensitivity across all elements. Method precision and accuracy were evaluated using procedural blanks and fortified samples prepared with standard solutions. The coefficient of variation (%CV) was ≤ 10% for all analytes, indicating excellent repeatability. Recovery values ranged from 85 to 115% for spiked blanks and 82–114% for fortified samples, all within the acceptable range of 80–120%, thereby confirming the reliability and trueness of the method in accordance with Instituto Nacional de Metrologia, Qualidade e Tecnologia guidelines.

2.11 Statistical analysis

Statistical analyses of antioxidant capacity, total phenolic content, and proximate composition were performed using R software (version 3.5.1). Data were analyzed by one-way analysis of variance (one-way ANOVA), considering each treatment condition as an independent group. When significant differences were detected, treatment means were compared using Fisher's least significant difference (LSD) test with Bonferroni adjustment at a significance level of 5% ($p \leq 0.05$), using the agricolae package. Different superscript lowercase letters indicate statistically significant differences among treatments. Data are presented as mean ± standard deviation, as indicated in the corresponding tables.

Mineral composition was analyzed separately using a two-way factorial ANOVA, considering ultrasound amplitude (20, 40, and 70%) and processing time (4, 8, and 12 min) as fixed factors, including the amplitude × time interaction. The untreated sample (B) was not included in the 3 × 3 factorial model and was used as the reference control in two-sided Dunnett comparisons with each ultrasound-treated condition. For each factorial effect, p-values obtained across the analyzed minerals were adjusted using the Benjamini–Hochberg false discovery rate procedure. Effect sizes were expressed as total eta squared (η^2), partial eta squared (partial η^2), and omega squared (ω^2). Dunnett-adjusted p-values were calculated within each mineral, and an additional Benjamini–Hochberg correction across all treatment-versus-control contrasts was applied as a conservative assessment of multiple comparisons. Mineral data are presented as mean, standard deviation, and coefficient of variation (CV%) from duplicate determinations ($n = 2$), with descriptive statistics for macro- and microminerals provided in Supplementary Tables S1A and S1B, respectively. Statistical significance was established at $p \leq 0.05$. Mineral analyses were performed in Python 3.13 using *SciPy* and *statsmodels*, and the complete results are presented in Supplementary Tables S1C and S1D.

3 Results and discussion

3.1 Theacrine mass spectrometric identification

The LC–ESI–QTOF-MS analysis of theacrine ($C_9H_{12}N_4O_3$) performed in positive ionization mode generated high-resolution mass spectral data, enabling reliable structural confirmation based on accurate mass determination and characteristic fragmentation pathways (Fig. 1). The protonated molecular ion $[M+H]^+$ was detected at m/z 225.0987, corresponding to the elemental composition $C_9H_{13}N_4O_3^+$, in excellent agreement with the theoretical exact mass (mass error, $\Delta = -0.4$ ppm). The low mass deviation obtained confirms the high analytical accuracy of the QTOF system and supports the unequivocal identification of theacrine in the analyzed sample.

The fragmentation pattern was characterized by a prominent ion at m/z 210.0753, corresponding to the neutral loss of a methyl radical (•CH_3, 15.0234 Da), yielding the ion $C_8H_{10}N_4O_3^+$ ($\Delta = 0.0$ ppm). Further fragmentation of the protonated molecular ion led to the formation of m/z 168.0769, attributed to the neutral loss of a CNO moiety (41.9980 Da), corresponding to $C_7H_{10}N_3O_2^+$ ($\Delta = -2.3$ ppm). Additionally, the fragment ion at m/z 153.0527 was observed and assigned to $C_6H_7N_3O_2^+$ ($\Delta = -7.2$ ppm), resulting from a subsequent methyl radical loss from the ion at m/z 168.0769 [10].

The identity of theacrine in the sample was further confirmed by the injection of an authentic standard in the HPLC-DAD system, which exhibited identical retention time and a characteristic absorption band at 292 nm, consistent with the UV–Vis profile of theacrine.

The quantitative results demonstrated variation in theacrine concentration among samples subjected to different ultrasound amplitudes, indicating that acoustic energy significantly influenced the extraction and availability of this alkaloid (Fig. 2). The sample treated with the highest ultrasound amplitude (C70/12) showed the greatest theacrine content compared to the control and lower amplitude treatments, suggesting that increased acoustic energy enhanced cavitation phenomena, promoting greater cell disruption and improved mass transfer of intracellular compounds. Ultrasound-assisted extraction has been widely reported as an efficient technique to increase the recovery of alkaloids and other bioactive molecules due to mechanical effects such as microjet formation, shear forces, and disruption of cell walls [39].

Although C70/12 exhibited the highest extraction efficiency, the response of samples submitted to lower amplitude conditions was not linear. In particular, samples from the 20% and 40% amplitude series (C20/4, C20/12, and C40/4) showed lower theacrine concentrations compared with the control or with higher amplitude treatments. This behavior suggests that insufficient acoustic energy or inadequate combinations of amplitude and processing time may not provide optimal cavitation conditions for effective disruption of plant tissues and release of intracellular metabolites. Additionally, prolonged exposure under suboptimal amplitude conditions may promote

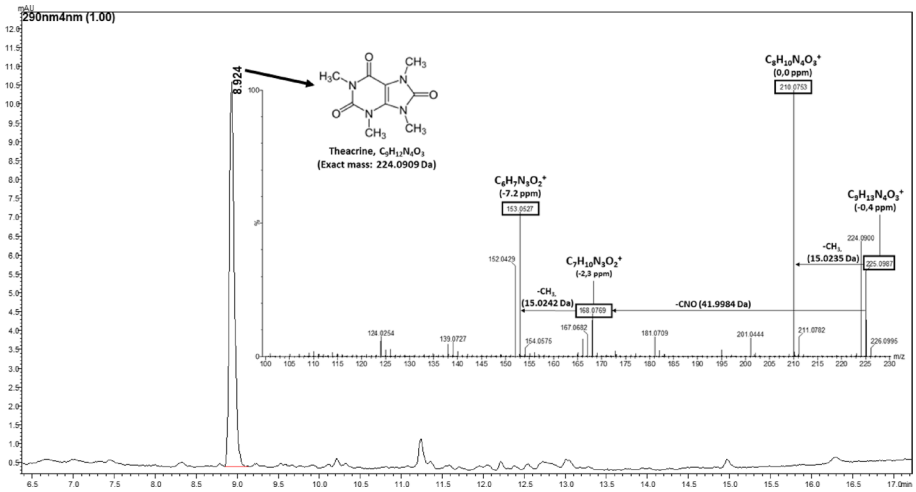


Fig. 1 High-resolution ESI(+)-QTOF mass spectrum of theacrine, highlighting the protonated molecular ion and main fragment ions formed via sequential neutral losses

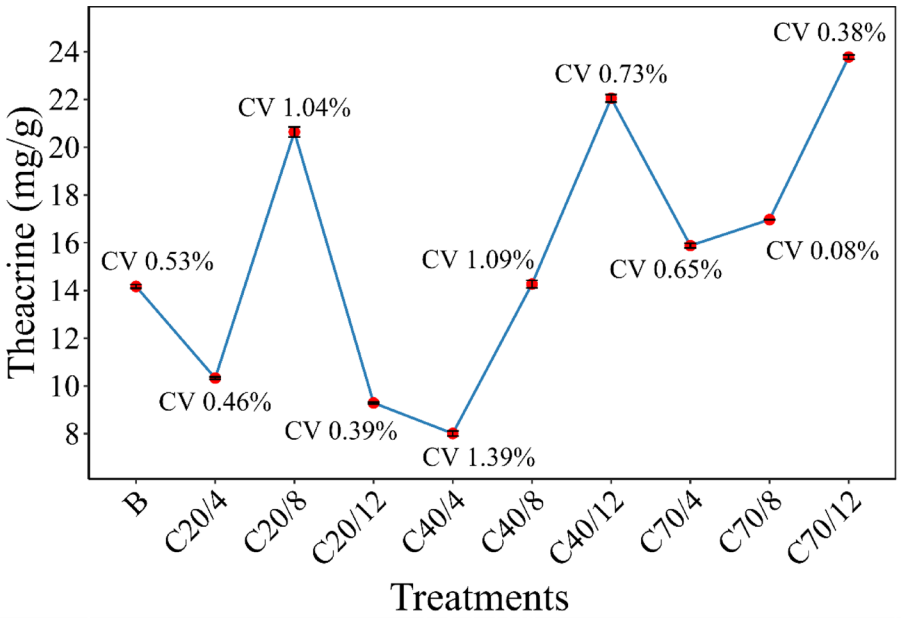


Fig. 2 Comparison of theacrine concentration in samples treated with different ultrasound amplitudes (20, 40 and 70%) for 4, 8 and 12 min, plus the control, determined by LC–ESI–QTOF-MS. CV values indicate the coefficient of variation (%), representing the relative dispersion of replicate measurements

localized thermal effects, oxidative reactions, or structural changes that limit the availability of theacrine, resulting in reduced extraction efficiency. Therefore, the relationship between ultrasound amplitude, processing time, and compound recovery appears to depend on achieving a suitable balance between cell disruption and preservation of bioactive compounds.

The lower theacrine concentration observed in C40/4 may be associated with limited structural disruption of plant tissues, resulting in reduced release of intracellular alkaloids. Lower ultrasound amplitude generates weaker cavitation intensity, which may be insufficient to disrupt the structural barriers that protect nitrogen-containing secondary metabolites. Previous studies have demonstrated that ultrasound amplitude and acoustic power influence cavitation bubble formation and collapse intensity, thereby affecting extraction efficiency of alkaloids, phenolic compounds, and other bioactive molecules [44]. It is important to note that amplitude and frequency represent distinct physical parameters in ultrasound-assisted extraction. While amplitude is related to the intensity of mechanical oscillation and delivered acoustic energy, frequency refers to the number of acoustic cycles per second. In conventional laboratory ultrasonic processors, frequency is generally maintained constant; therefore, differences among treatments in the present study are primarily associated with variations in ultrasound amplitude.

Previous research evaluating ultrasound-assisted extraction of bioactive compounds from plant matrices reported increased recovery when higher acoustic power or optimized exposure times were applied. These effects are attributed to enhanced solvent penetration, improved diffusion kinetics, and increased desorption of compounds associated with structural components such as cellulose and proteins. Similar behavior has been observed for caffeine and structurally related purine alkaloids, where ultrasound pretreatment improves extraction efficiency compared with conventional extraction techniques [47].

The higher concentration of theacrine observed in the sample treated at greater amplitude may also be related to partial modification of intermolecular interactions between alkaloids and macromolecules, such as polysaccharides and proteins. Ultrasound treatment can weaken hydrogen bonding interactions and increase accessibility of compounds located within cellular compartments. The structural disruption observed in SEM images supports this interpretation, demonstrating increased porosity and reduced particle compactness in samples subjected to higher acoustic energy [9].

Conversely, excessively intense ultrasound conditions may also promote degradation of thermolabile compounds depending on exposure time and energy density. However, the preservation of theacrine structure observed

in chromatographic profiles suggests that the applied conditions did not induce significant chemical degradation, indicating that the selected parameters were adequate to maximize extraction efficiency while maintaining molecular integrity. Similar findings have been reported for ultrasound-assisted extraction of alkaloids from tea and guarana matrices [31].

Overall, the results indicate that ultrasound amplitude plays a decisive role in determining the concentration of theacrine, with higher acoustic energy favoring compound release through intensified cavitation effects. However, the effectiveness of ultrasound treatment depends on the optimization of amplitude and processing time, since insufficient or excessive energy input may reduce extraction performance. These findings confirm the potential of ultrasound technology as an efficient strategy to enhance the recovery of purine alkaloids from plant matrices, contributing to the optimization of extraction processes for functional ingredients derived from Amazonian species.

3.2 Effect of ultrasound treatment on antioxidant activity

Table 1 presents the antioxidant activity of *cacauí* seed powder subjected to different ultrasound pretreatment conditions, evaluated using the DPPH, ABTS, and FRAP assays, together with the total phenolic content (TPC). Overall, ultrasound pretreatment significantly affected the antioxidant capacity of the samples, demonstrating that both ultrasound amplitude and processing time strongly influenced the extraction of phenolic compounds and other bioactive constituents from the seed matrix through acoustic cavitation.

Samples subjected to higher ultrasound amplitudes generally exhibited greater antioxidant activity and total phenolic content, particularly when combined with longer processing times. Among all treatments, **C70/12** produced the highest values for all evaluated parameters (DPPH = 1549.3 µM Trolox/mL; ABTS = 2035.2 µM Trolox/mL; TPC = 293.6 mg GAE/mL; FRAP = 1395.0 µM Fe(II)/mL), indicating that the combination of 70% amplitude and 12 min was the most effective condition for promoting the release of antioxidant compounds. These results suggest that higher acoustic energy intensified cavitation phenomena, generating stronger shear forces and microjets that enhanced cell wall disruption, solvent penetration, and mass transfer, thereby increasing the extraction efficiency of phenolic compounds and other reducing metabolites [45].

The influence of ultrasound pretreatment, however, was not linear across all experimental conditions. At 20% amplitude, increasing the processing time from 8 to 12 min resulted in a marked decrease in all antioxidant parameters. DPPH values decreased from 1299.3 to 706.1 µM Trolox/mL, while ABTS, FRAP, and TPC exhibited

Table 1 Effect of ultrasound pretreatment on antioxidant capacity (DPPH, ABTS, FRAP) and total phenolic content of cacauí seed powders

Samples	DPPH (µMTrolox/mL)	ABTS (µMTrolox/mL)	TPC (mgGAE/mL)	FRAP (µMFe(II)/mL)
B	825.2 ± 6.2^{g}	1074.1 ± 6.9^{g}	38.9 ± 1.1^{g}	920.6 ± 3.9^{g}
C20/4	761.0 ± 6.6^{h}	898.5 ± 10.1^{h}	22.1 ± 1.2^{h}	732.1 ± 1.7^{h}
C20/8	1299.3 ± 6.2^{c}	1834.1 ± 8.3^{c}	163.1 ± 5.5^{c}	1239.5 ± 1.7^{c}
C20/12	706.1 ± 6.2^{j}	834.1 ± 8.3^{i}	14.3 ± 0.8^{i}	698.7 ± 3.9^{i}
C40/4	582.7 ± 3.8^{i}	737.4 ± 8.3^{j}	10.9 ± 0.8^{j}	673.9 ± 3.6^{j}
C40/8	950.2 ± 6.2^{f}	1267.4 ± 10.1^{f}	85.0 ± 1.0^{f}	940.2 ± 2.9^{f}
C40/12	1501.8 ± 5.2^{b}	1966.3 ± 6.6^{b}	227.2 ± 0.7^{b}	1260.6 ± 3.9^{b}
C70/4	1080.2 ± 5.2^{e}	1438.5 ± 10.7^{e}	131.6 ± 0.5^{e}	1017.6 ± 1.7^{e}
C70/8	1105.2 ± 5.2^{d}	1561.8 ± 8.4^{d}	145.8 ± 1.0^{d}	1053.2 ± 2.8^{d}
C70/12	1549.3 ± 8.8^{a}	2035.2 ± 10.1^{a}	293.6 ± 0.9^{a}	1395.0 ± 2.8^{a}

Values are expressed as mean ± standard deviation ($n = 3$). Means followed by different superscript lowercase letters within the same column are significantly different according to one-way analysis of variance (ANOVA) followed by Fisher's Least Significant Difference (LSD) test with Bonferroni adjustment ($p \leq 0.05$). Means sharing at least one identical superscript letter are not significantly different ($p > 0.05$). B: untreated control. CX/Y: ultrasound-treated sample, where C denotes the coded sample, X represents the ultrasound amplitude (%) and Y represents the processing time (min). Ultrasound amplitude refers to the acoustic amplitude of the ultrasonic probe, expressed as a percentage of the maximum displacement of the probe tip

similar reductions. This behavior indicates that extending the treatment time under low acoustic amplitude did not provide sufficient cavitation intensity to sustain the extraction process. Instead, prolonged sonication at low energy may have promoted oxidation or degradation of readily extractable phenolic compounds through prolonged exposure to reactive oxygen species generated during cavitation, while the limited mechanical disruption was insufficient to release additional intracellular compounds. Similar non-linear responses have been reported in ultrasound-assisted extraction studies, demonstrating that extraction efficiency depends on an appropriate balance between ultrasound intensity and treatment duration rather than simply increasing processing time [6].

A different trend was observed at 40% amplitude. Although the shortest treatment (C40/4) produced the lowest antioxidant values among all samples, increasing the processing time progressively improved antioxidant activity, with C40/12 exhibiting substantial increases in DPPH, ABTS, FRAP, and TPC compared with both the untreated control and the shorter treatments. These findings indicate that an intermediate acoustic amplitude required longer exposure to accumulate sufficient cavitation effects capable of effectively disrupting the seed matrix and promoting the release of bound phenolic compounds.

The 70% amplitude treatments exhibited the most consistent behavior. Antioxidant activity and total phenolic content increased progressively from C70/4 to C70/8 and reached their maximum values at C70/12, demonstrating that higher ultrasound amplitudes combined with longer treatment times maximized extraction efficiency. Unlike the response observed at 20% amplitude, the higher acoustic energy generated under 70% amplitude appeared sufficient to maintain effective cavitation throughout the treatment, continuously enhancing cell disruption and mass transfer without evidence of significant degradation of antioxidant compounds. These results demonstrate that the interaction between ultrasound amplitude and processing time plays a decisive role in determining extraction efficiency.

These findings are consistent with those of Kumar et al. [24], who observed that increasing ultrasonic power improved the extraction efficiency of phenolic compounds by increasing particle surface area and facilitating solvent penetration into the plant matrix. However, the reduced antioxidant activity observed under some lower-energy treatments in the present study suggests that ultrasound efficiency depends on the appropriate combination of processing parameters, highlighting that insufficient acoustic energy may not be adequate to promote effective cell disruption.

The total phenolic content closely followed the trends observed for DPPH, ABTS, and FRAP, confirming the strong relationship between phenolic compounds and antioxidant activity. Phenolic acids and flavonoids possess hydroxylated aromatic structures capable of donating electrons and stabilizing free radicals, making them major contributors to the antioxidant capacity of plant-derived materials [38]. Likewise, the FRAP assay showed a pattern consistent with the radical scavenging assays, indicating that the increased reducing power of the extracts resulted primarily from the enhanced extraction of phenolic compounds.

The FRAP assay showed a trend similar to the DPPH and ABTS methods, confirming that increasing ultrasound intensity enhanced the reducing capacity of the extracts. Studies have demonstrated that ultrasonic treatments can improve the reducing power of plant extracts due to the enhanced release of phenolic compounds bound to the lignocellulosic matrix [45].

Overall, the results demonstrate that ultrasound pretreatment is an effective strategy for improving the antioxidant properties of *Theobroma speciosum* seed powder. However, the effectiveness of the process depends on the appropriate combination of ultrasound amplitude and treatment time. While insufficient acoustic energy limited extraction efficiency and, under some conditions, prolonged sonication even reduced antioxidant activity, higher amplitudes consistently enhanced the recovery of bioactive compounds. Under the conditions evaluated, 70% ultrasound amplitude combined with 12 min of treatment provided the highest extraction of phenolic compounds and antioxidant activity, highlighting ultrasound pretreatment as a sustainable and efficient technology for the valorization of underutilized Amazonian plant resources and the development of functional food ingredients.

3.3 Proximate composition

The analyzed cacauí seed powder samples comprise both the untreated control (B) and the ultrasound-pretreated samples (C20/4, C20/8, C20/12, C40/4, C40/8, C40/12, C70/4, C70/8, and C70/12). Accordingly, all values reported in this section and in Table 2 refer to both the raw material prior to treatment (control) and after ultrasound pretreatment under the different conditions applied.

Overall, the proximate composition of cacauí seed powder revealed low moisture content (2.31–3.98%), high lipid content (25.94–28.92%), moderate protein levels (14.69–16.25%), and a predominance of carbohydrates (50.31–54.37%), along with ash content ranging from 1.78 to 2.85%. These findings highlight the nutritional and technological potential of this raw material, particularly for use as a functional ingredient or as a source of bioactive compounds (Table 2).

The low moisture content observed in all samples is a positive factor for product stability, as it reduces water activity and, consequently, susceptibility to microbial growth and chemical degradation during storage. Studies on seeds from species of the genus *Theobroma* have shown that reduced moisture contributes to greater stability of phenolic and lipid compounds, preserving antioxidant and nutritional properties [22].

The lipid content found in the samples (26–29%) is characteristic of seeds from the genus *Theobroma*, which present high concentrations of fatty acids, particularly oleic and stearic acids, associated with energy storage and relevant technological properties, such as texture and oxidative stability [5]. Similar lipid and protein values have been reported for cocoa seeds, indicating that these raw materials have potential as a source of vegetable fat with applications in the food industry [14].

The protein content (14.69–16.25%) falls within the range reported for *Theobroma* seeds, which may present values close to 15% on a dry basis, contributing to the nutritional and functional value of the product [29]. Proteins present in these seeds play an important role in metabolic processes and may contribute to technological properties, such as water retention and emulsification capacity in food systems.

The carbohydrate fraction was predominant (50–54%), indicating that the seed powder has potential as an energy source. The predominance of carbohydrates in plant matrices is also associated with the presence of structural fibers and polysaccharides that influence functional characteristics, such as water absorption capacity and stability of colloidal systems [14].

The ash content (1.78–2.85%) indicates the presence of minerals important for human metabolism and the nutritional value of the food. The mineral composition of species from the genus *Theobroma* includes essential elements such as potassium, magnesium, and iron, which contribute to functional and nutritional properties [22].

Taken together, the proximate composition results indicate that cacauí seed powder maintained a broadly similar nutritional profile across the ultrasound treatments. Although statistically significant differences were

Table 2 Proximate composition of the samples (%)

Sample	Moisture (%)	Ash (%)	Lipids (%)	Proteins (%)	Carbohydrates (%)
B	3.16 ± 0.01^{e}	2.66 ± 0.01^{b}	26.63 ± 0.01^{i}	14.89 ± 0.03^{f}	52.67 ± 0.03^{b}
C20/4	3.34 ± 0.01^{d}	2.41 ± 0.01^{de}	28.92 ± 0.02^{a}	15.01 ± 0.01^{de}	50.31 ± 0.02^{j}
C20/8	2.31 ± 0.01^{h}	2.33 ± 0.01^{f}	25.94 ± 0.01^{j}	15.05 ± 0.03^{d}	54.37 ± 0.01^{a}
C20/12	2.40 ± 0.02^{g}	2.27 ± 0.03^{g}	27.57 ± 0.01^{g}	16.25 ± 0.02^{a}	51.51 ± 0.00^{c}
C40/4	3.03 ± 0.03^{f}	1.78 ± 0.01^{i}	28.23 ± 0.01^{d}	15.53 ± 0.00^{b}	51.43 ± 0.03^{d}
C40/8	3.62 ± 0.01^{b}	2.16 ± 0.01^{h}	28.86 ± 0.03^{b}	14.69 ± 0.01^{g}	50.66 ± 0.04^{h}
C40/12	3.98 ± 0.01^{a}	2.37 ± 0.02^{ef}	27.34 ± 0.02^{h}	14.98 ± 0.01^{e}	51.33 ± 0.03^{e}
C70/4	3.13 ± 0.02^{e}	2.43 ± 0.01^{d}	28.68 ± 0.01^{c}	15.32 ± 0.00^{c}	50.44 ± 0.02^{i}
C70/8	3.16 ± 0.01^{e}	2.57 ± 0.01^{c}	28.02 ± 0.01^{e}	15.29 ± 0.00^{c}	50.96 ± 0.01^{f}
C70/12	3.52 ± 0.02^{c}	2.85 ± 0.01^{a}	27.87 ± 0.01^{f}	15.02 ± 0.02^{de}	50.75 ± 0.03^{g}

Values are expressed as mean ± standard deviation ($n = 3$). Different superscript letters within the same column indicate statistically significant differences among treatments according to one-way ANOVA followed by Fisher's LSD test with Bonferroni adjustment ($p \leq 0.05$). Carbohydrate content was calculated by difference. B: untreated control; CX/Y: ultrasound-treated sample, where X indicates ultrasound amplitude (%) and Y indicates processing time (min)

observed among treatments for moisture, ash, lipid, protein, and total carbohydrate contents, these data should be interpreted cautiously. Proximate composition analyses quantify bulk nutritional fractions and do not provide direct evidence of chemical transformation of macronutrients by ultrasound. Therefore, the observed differences are more appropriately interpreted as small compositional fluctuations, potentially associated with changes in water retention, particle disruption, extraction efficiency, and sample heterogeneity, rather than as evidence of substantial macronutrient degradation or conversion.

The results demonstrate that cacauí seed powder presents a nutritional composition similar to that reported for other species of the genus, highlighting its potential as a promising source of lipids, proteins, and bioactive compounds with potential application in the functional food industry.

3.4 Fourier transform infrared spectroscopy (FTIR)

Fourier transform infrared spectroscopy (FTIR) was used for the structural characterization of cacauí seed powder, enabling the identification of functional groups associated with the main chemical constituents of the sample (Fig. 3).

The absorption bands in the regions of 2922–2914 cm^{-1} and 2855–2847 cm^{-1} were attributed to asymmetric and symmetric C–H stretching vibrations of aliphatic chains, typical of fatty acids and triglycerides present in lipid-rich seeds. These bands exhibited a gradual decrease in intensity with increasing ultrasound amplitude, being more pronounced in the 40% and 70% treatments, suggesting reduced structural order or increased accessibility of lipid domains due to cavitation effects. Similar spectral features have been reported in cocoa matrices, where peaks around 2920 and 2850 cm^{-1} are associated with lipids and related compounds formed during processing [7].

The presence of an intense band at 1736 cm^{-1} is associated with the stretching vibration of the C = O bond of ester groups, indicating the presence of triacylglycerols and other structural lipid compounds. Similar results

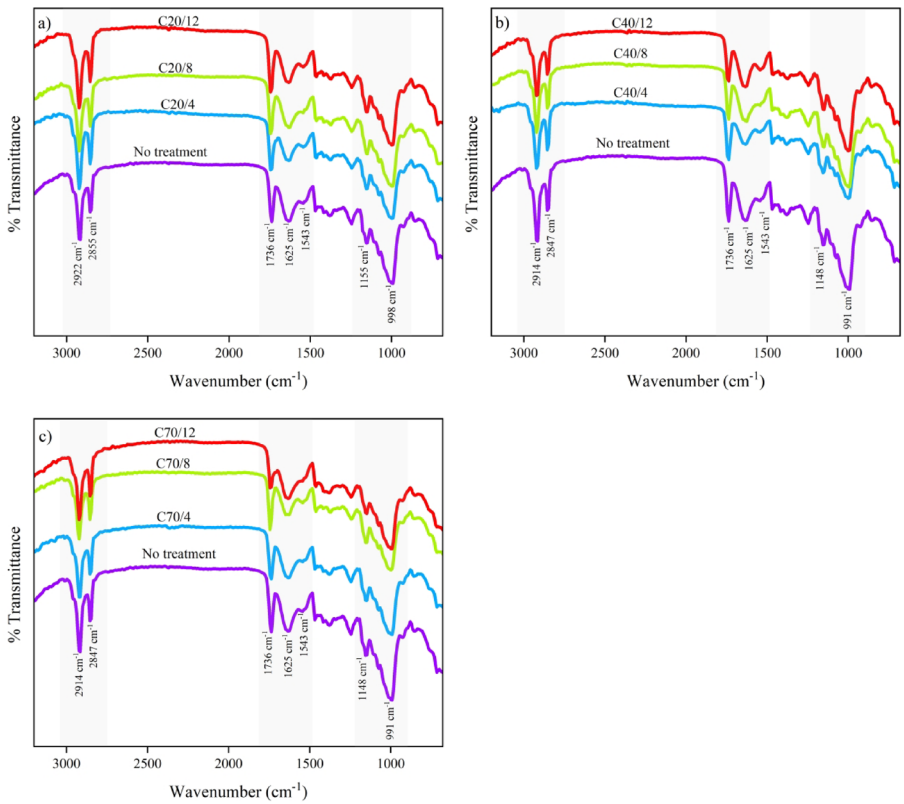


Fig. 3 Fourier transform infrared (FTIR) spectra of cacauí (*Theobroma speciosum*) seed powder subjected to ultrasound pretreatment at different amplitudes (20, 40, and 70%) and processing times (4, 8, and 12 min), compared with the untreated control sample

have been reported in FTIR analyses of cocoa and chocolate, where bands in the 1745–1730 cm^{-1} region were attributed to lipids and phenolic-derived compounds [36].

In the protein-related region, the amide I band (~1625 cm^{-1}), corresponding mainly to C = O stretching vibrations of peptide bonds, exhibited subtle intensity changes across treatments, with a more noticeable decrease in the most intense ultrasound conditions (C40 and C70). This behavior suggests alterations in protein secondary structure environment and intermolecular interactions. This region may also overlap with signals from conjugated phenolic compounds and flavonoids, which contribute to the antioxidant properties of the matrix. FTIR studies in cocoa systems have similarly associated this range (1616–1690 cm^{-1}) with proteins, phenolics, and Maillard reaction products.

The amide II band (~ 1543 cm^{-1}), related to N–H bending and C–N stretching vibrations, followed a comparable trend, with slight intensity attenuation under stronger ultrasound treatments. This suggests modifications in protein conformation and hydrogen-bonding networks rather than breakdown of protein structures. Similar spectral responses have been reported in cocoa beans, where this region is associated with protein structure and aromatic compounds influencing functional Properties [27].

In the carbohydrate region (1148–991 cm^{-1}), attributed to C–O and C–O–C stretching vibrations of polysaccharides such as cellulose and hemicellulose, a more pronounced decrease in band intensity was observed under higher ultrasound amplitudes, particularly in the C70 treatment. This suggests partial disruption of the plant cell wall matrix, increasing the exposure of structural polysaccharides and potentially enhancing mass transfer phenomena. This region is commonly associated with the structural framework of cocoa seeds and related plant matrices rich in glucose, fructose, and sucrose derivatives [7].

Overall, the comparative analysis across ultrasound treatments (20, 40, and 70% amplitude) indicates a clear intensity-dependent effect, with more pronounced spectral changes observed at higher amplitudes and longer processing times. These variations suggest that ultrasound-induced cavitation promotes structural rearrangements in the plant matrix, affecting intermolecular interactions without altering the fundamental chemical structures, as no new absorption bands or significant peak shifts were detected.

Ultrasound pretreatment thus promoted subtle but systematic modifications in the chemical matrix of cacauí seed powder, preserving the main functional groups associated with lipids, proteins, and carbohydrates while enhancing structural accessibility. This behavior is consistent with emerging processing technologies that aim to improve the release of bioactive compounds through physical restructuring mechanisms rather than chemical degradation.

3.5 Structural disruption observed in SEM images

Scanning electron microscopy (SEM) micrographs (Fig. A–J) reveal significant morphological differences between the untreated sample and those subjected to ultrasound pre-treatment at different amplitudes (20, 40, and 70%) and processing times (4, 8, and 12 min). The structural modifications observed in the particles indicate that acoustic cavitation promoted progressive disruption of the plant matrix, which may influence the extraction of bioactive compounds and the functional properties of the powder (Fig. 4).

The untreated sample (Fig. A – control) exhibits particles with irregular geometry, a relatively compact structure, and smooth surfaces, typical of plant matrices rich in lipids and polysaccharides. Similar morphologies have been reported for cocoa powder and other *Theobroma* species, which commonly present agglomerated particles due to interactions between lipids and proteins, forming cohesive structures [34].

After ultrasound treatment at 20% amplitude (Fig. B–D), structural modifications become evident. Sample C20/4 (Fig. B) shows the onset of surface roughness and partial particle fragmentation. At longer processing times, C20/8 and C20/12 (Fig. C and D) exhibit increased irregularity, pore formation, and partial disintegration of agglomerates. Ultrasonic waves generate cavitation bubbles that collapse near the particle surface, producing localized high pressure and temperature, which promotes cell wall disruption and increases porosity [43].

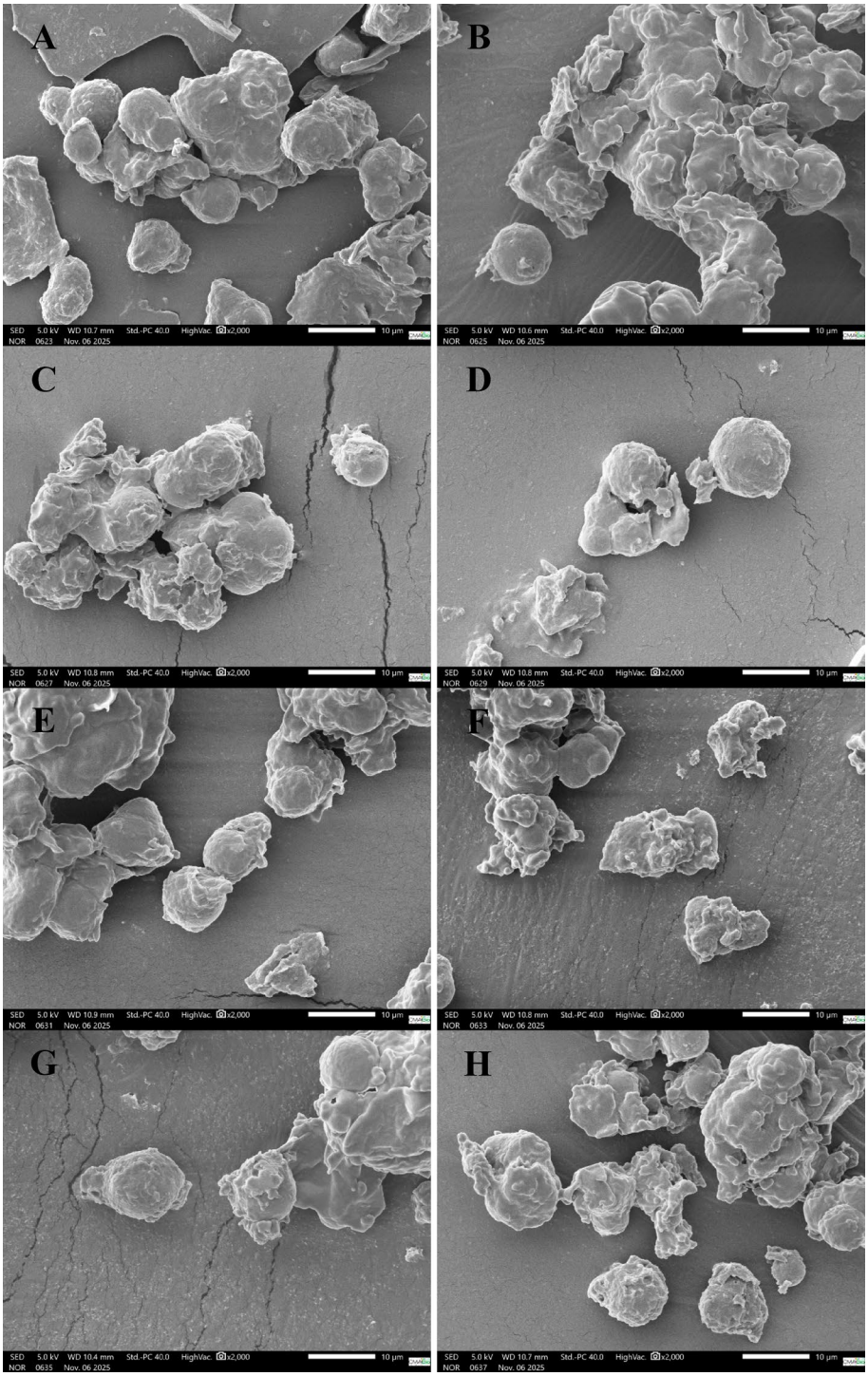


Fig. 4 Scanning electron microscopy (SEM) micrographs of cacauí (*Theobroma speciosum*) seed powder. **A** Untreated control (B); (**B**–**D**) ultrasound-treated samples at 20% amplitude for 4, 8, and 12 min (C20/4, C20/8, and C20/12, respectively); (**E**–**G**) ultrasound-treated samples at 40% amplitude for 4, 8, and 12 min (C40/4, C40/8, and C40/12, respectively); (**H**–**J**) ultrasound-treated samples at 70% amplitude for 4, 8, and 12 min (C70/4, C70/8, and C70/12, respectively)

For treatments at 40% amplitude (Fig. E–G), structural disruption becomes more pronounced. The particles appear less compact and more fragmented, indicating greater mechanical stress promoted by ultrasonic energy. The formation of fissures and irregular surfaces suggests structural weakening of the cellular matrix. Studies have shown that ultrasound processing can significantly modify plant microstructure, promoting the rupture of parenchymal cells and facilitating solvent penetration [15].

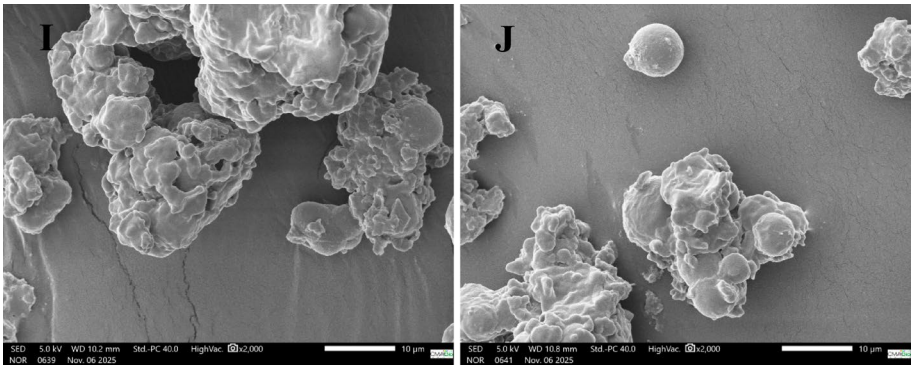


Fig. 4 (continued)

At 70% amplitude (Fig. H–J), more intense morphological changes are observed, characterized by greater fragmentation, rougher surfaces, and a reduction in particle size. The C70/12 sample (Fig. J) shows clear structural collapse and the formation of smaller aggregates, indicating a higher intensity of cavitation effects. According to Prempeh et al. [33], higher ultrasound amplitudes increase shear forces and microjet formation, promoting disruption of plant tissues and enhancing the release of intracellular compounds such as phenolics and lipids.

The progressive increase in structural disorganization observed with increasing amplitude and processing time confirms that ultrasound affects the integrity of the plant matrix. A similar behavior has been reported for *Pouteria lucuma* seeds, where ultrasound treatment promoted particle size reduction and increased surface area, improving the extraction efficiency of bioactive compounds [28].

The morphological changes observed in the SEM images are consistent with the FTIR and antioxidant results, suggesting that ultrasound promoted structural modifications capable of increasing the accessibility of phenolic compounds. Prempeh et al. [33] reported that the development of porous structures and the reduction in particle size can enhance solvent penetration and improve mass transfer efficiency during extraction processes, thereby facilitating the release of intracellular compounds.

3.6 Thermogravimetric analysis

The TG and DTG curves of the untreated sample (No treatment) were considered as the reference baseline for evaluating the thermal behavior changes induced by ultrasound pretreatment (Fig. 5). Only the samples treated for 12 min (C20/12, C40/12, and C70/12) were included in Fig. 5 because this processing time produced the most pronounced physicochemical and microstructural modifications observed throughout the study, as evidenced by the chemical composition, antioxidant activity, and SEM analyses. Presenting only the 12-min treatments allows a clearer comparison of the effect of ultrasound amplitude on the thermal degradation profile while avoiding excessive overlap among TG and DTG curves, which would hinder visualization if all treatments were simultaneously displayed. Compared with this control profile, the ultrasound-treated samples exhibited variations in mass loss patterns and degradation stages, indicating that acoustic treatment modified the thermal response of the lignocellulosic matrix. The TG and DTG curves showed a degradation profile typical of lignocellulosic biomasses and oilseed matrices, characterized by three main stages of mass loss associated with moisture evaporation and decomposition of structural macromolecules (Fig. 5). Similar thermal behavior has been reported for cocoa byproducts, which present complex matrices composed of lipids, proteins, cellulose, and lignin [20].

The first degradation stage, observed between approximately 25 and 150 °C, showed mass losses ranging from 4.29 to 8.38%, corresponding to the evaporation of free and bound water, as well as low molecular weight volatile compounds. Relative to the untreated control, ultrasound-treated samples showed differences in moisture-related mass loss, particularly C20/12 and C70/12, suggesting modifications in water retention capacity due to microstructural disruption caused by cavitation effects. Similar results have been reported for plant biomasses

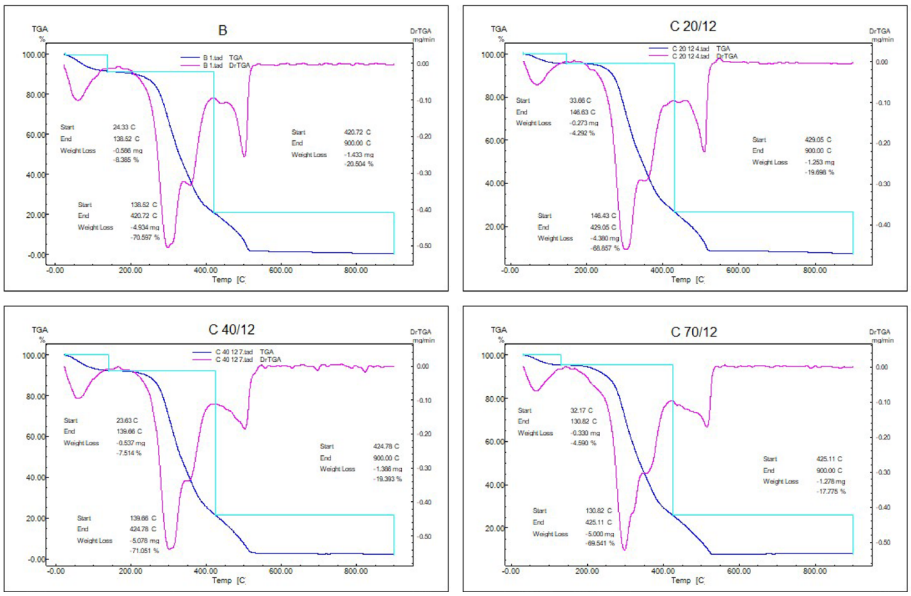


Fig. 5 Thermogravimetric (TG) and derivative thermogravimetric (DTG) curves of cacauí (*Theobroma speciosum*) seed powder: untreated control sample (B) and ultrasound-treated samples at amplitudes of 20, 40, and 70% and processing times of 4, 8, and 12 min

subjected to physical pretreatments, in which structural modifications reduced hydrogen bonding interactions between water molecules and polysaccharides [40].

The second stage of thermal degradation, occurring between 130 and 430 °C, corresponded to the main mass loss event (approximately 68–71%) and was associated with the decomposition of hemicellulose, cellulose, proteins, and lipids. Compared with the untreated sample, the treated materials exhibited slight differences in degradation intensity, reflecting modifications in the accessibility and organization of structural components after ultrasound exposure. The DTG peaks observed between 280 and 350 °C indicate maximum degradation rates of these macromolecules, consistent with thermal profiles reported for cocoa shells, cupuaçu seeds, and other lignocellulosic materials [3].

The third degradation stage, observed between 420 and 900 °C, with mass losses ranging from 17.77 to 20.50%, was associated with lignin decomposition and the formation of carbonaceous residues. Lignin exhibits high thermal stability due to its complex aromatic structure, resulting in gradual degradation over a wide temperature range [11]. Compared with the untreated control, the slightly lower mass loss observed for sample C70/12 suggests increased thermal stability, possibly related to structural rearrangements promoted by ultrasound treatment. Similar behavior has been observed in oilseed cakes and cocoa residues, where physical pretreatments influence pyrolysis pathways and char formation [35].

Overall, the comparison with the untreated sample demonstrates that ultrasound pretreatment altered the thermal degradation profile of cacauí seed powder, with the extent of modification depending on the applied amplitude and processing time. The treatment at 70% amplitude for 12 min promoted the greatest structural modification, reflected by increased particle irregularity and a slight improvement in thermal stability during the final degradation phase. The combined analytical approach confirms that cavitation effects modify the organization of the lignocellulosic matrix, facilitating heat transfer and altering degradation intensity while preserving the chemical integrity of the material. These findings suggest that ultrasound pretreatment represents a promising strategy to modify the physicochemical properties of cacauí seed powder, potentially improving its applicability in food, pharmaceutical, and biotechnological processes.

3.7 Determination of macro- and microminerals by inductively cacauí seed powder optical emission spectroscopy (ICP-OES)

The mineral profile of cacauí seed powder obtained after ultrasound pretreatment revealed that potassium (K), phosphorus (P), magnesium (Mg), and calcium (Ca) were the predominant macrominerals, whereas iron (Fe), zinc (Zn), manganese (Mn), and copper (Cu) were detected as minor elements (Figs. 6 and 7). The results indicate that ultrasound pretreatment did not markedly modify the qualitative mineral profile of cacauí seeds, since the same major and trace elements were detected in the analyzed samples. However, differences in mineral concentrations among treatments suggest that ultrasound-assisted processing may influence the extractability or distribution of inorganic compounds within the seed matrix.

The two-way ANOVA revealed significant effects of ultrasound amplitude, processing time, and their interaction on mineral concentrations after false discovery rate correction (Supplementary Table S1C). This interaction indicates that the mineral response depended on the specific combination of amplitude and treatment time. Dunnett comparisons identified C40/12 as the condition with the most pronounced overall decrease, with reductions ranging from 38.9 to 51.2%, whereas C20/8 produced moderate increases in several minerals, ranging from 11.3 to 15.9% (Supplementary Table S1D).

The predominance of K, P, Mg, and Ca observed in cacauí seed powder is consistent with the mineral composition commonly reported for species of the Theobroma genus. These elements are recognized as the main inorganic constituents of cocoa-related seeds, contributing to plant physiological functions and the nutritional value of derived ingredients. Similar profiles have been described for cocoa beans, where K, Mg, and P represent the major mineral fractions and are associated with osmotic regulation, enzymatic activation, energy metabolism, and structural stabilization of cellular components [32]. Therefore, the mineral pattern observed in the present study confirms the nutritional similarity between cacauí and other Amazonian Theobroma species.

The effect of ultrasound pretreatment on mineral composition should be considered in relation to its ability to promote structural disruption of plant tissues and improve mass transfer phenomena. Although ultrasound is

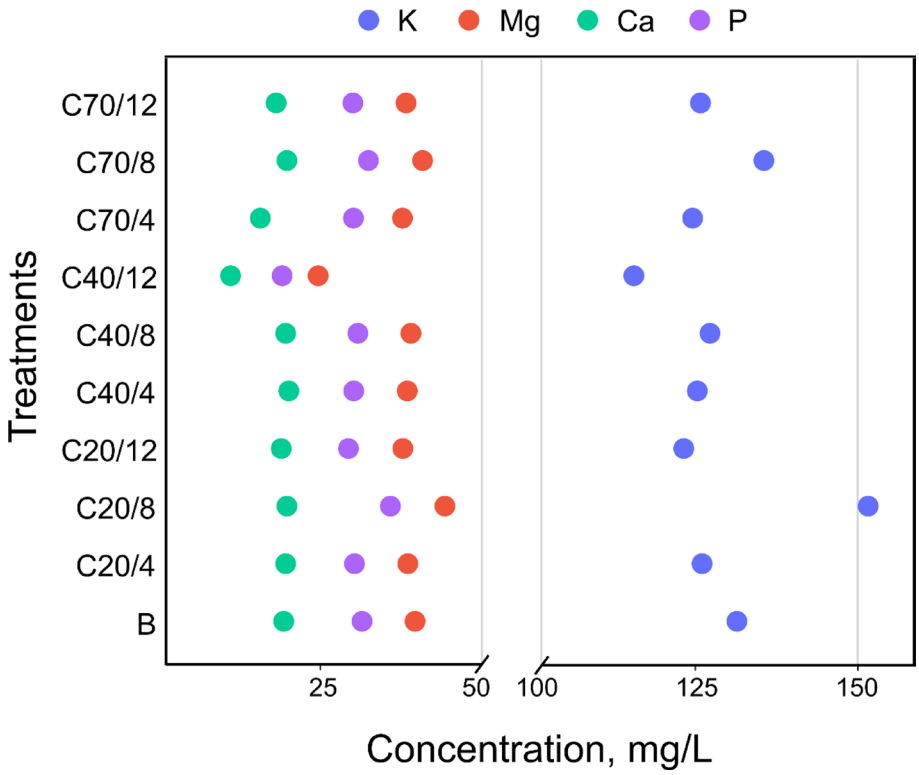


Fig. 6 Macromineral composition of cacauí seed powder determined by ICP-OES. The figure shows the concentrations of potassium (K), magnesium (Mg), calcium (Ca), and phosphorus (P) in the untreated control sample and in samples subjected to ultrasound pre-treatment at different amplitudes (20, 40, and 70%) and processing times (4, 8, and 12 min). Data points represent mean concentrations expressed in mg/L. B: untreated control; CX/Y: ultrasound-treated sample, where X indicates ultrasound amplitude (%) and Y indicates processing time (min). The corresponding mean, standard deviation, and coefficient of variation (CV%) values for all macrominerals are provided in Supplementary Table S1A

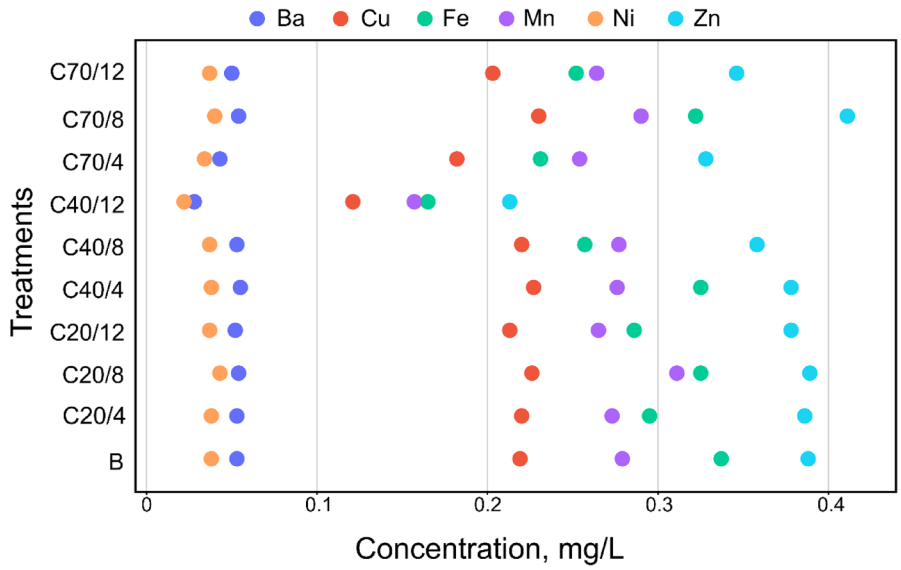


Fig. 7 Micromineral composition of cacauí seed powder determined by ICP-OES. The figure shows the concentrations of barium (Ba), copper (Cu), iron (Fe), manganese (Mn), nickel (Ni), and zinc (Zn) in the untreated control sample and in samples subjected to ultrasound pre-treatment at different amplitudes (20, 40, and 70%) and processing times (4, 8, and 12 min). Data points represent mean concentrations expressed in mg/L. B: untreated control; Cx/y: ultrasound-treated sample, where x indicates ultrasound amplitude (%) and y indicates processing time (min). The corresponding mean, standard deviation, and coefficient of variation (CV%) values for all microminerals are provided in Supplementary Table S1B

commonly applied to enhance the extraction of bioactive compounds, its influence on minerals may depend on matrix characteristics, treatment intensity, and interactions between minerals and organic components such as proteins, polysaccharides, and phenolic compounds.

The concentrations of K, Ca, Mg, and P found in cacauí seeds are comparable to those reported for cocoa cultivated under different environmental conditions. Previous studies have demonstrated that mineral accumulation in Theobroma species is influenced by genotype, soil composition, and plant development conditions, resulting in variability among samples [8]. Thus, differences between the present results and previous reports may be attributed not only to genetic variability among species but also to geographical origin and agricultural conditions.

Regarding micronutrients, Fe, Zn, Mn, and Cu were detected in the cacauí seed powder, indicating the presence of essential trace elements with potential nutritional relevance. These minerals participate as enzymatic cofactors in metabolic processes and antioxidant defense mechanisms, including the activity of enzymes such as superoxide dismutase and catalase. Similar microneral profiles have been reported for cocoa and cupuaçu seeds, in which Fe, Zn, and Cu contribute to the functional and nutritional characteristics of plant-derived ingredients [14]. The maintenance of these trace elements after ultrasound pretreatment further demonstrates the suitability of this processing strategy for obtaining mineral-rich cacauí ingredients.

Trace elements such as iron (Fe), zinc (Zn), manganese (Mn), and copper (Cu) were also detected (Fig. 7), demonstrating similarity with mineral profiles reported for cocoa beans subjected to fermentation and processing. These micronutrients act as cofactors of antioxidant enzymes, including superoxide dismutase and catalase, which play important roles in controlling oxidative reactions in plant tissues and food matrices. Studies indicate that fermentation and post-harvest treatments may influence mineral bioavailability, particularly Fe and Zn, without significantly altering total mineral concentrations [25].

From a nutritional perspective, the mineral composition obtained highlights the potential contribution of cacauí seed powder as a source of essential minerals. The presence of Mg and K may contribute to dietary mineral intake, considering the recommended daily requirements for adults, while Ca and P may provide additional

nutritional value in plant-based formulations. Although the contribution depends on the serving size and formulation, the mineral profile demonstrates the potential of Amazonian Theobroma species as sources of nutritionally relevant elements.

Overall, the results demonstrate that ultrasound pretreatment preserved the mineral composition of cacauí seed powder, maintaining the predominance of essential macro- and microminerals characteristic of Theobroma species. In addition to the essential elements, Fig. 7 also shows the presence of barium (Ba) and nickel (Ni) in all samples. Although these elements were detected at the analytical level, their occurrence should be interpreted according to their concentrations and potential implications for food safety. The detection of Ba and Ni may be related to natural mineral composition, environmental conditions, and soil characteristics, which can influence elemental uptake by plants. These findings reinforce the technological potential of ultrasound-assisted processing for producing nutritionally valuable cacauí-based ingredients while maintaining their mineral quality.

The mineral profile observed in cacao-related seeds is consistent with reports describing *Theobroma cacao* as an important source of essential macro- and microelements, including Ca, Mg, Zn, and Cu, which contribute to nutritional quality and potential functional benefits. Variability in mineral composition may be associated with soil characteristics, genetic factors, and environmental conditions during plant development. Furthermore, the accumulation of trace elements in cocoa plants has been shown to depend on mineral availability in the soil and plant uptake mechanisms [18].

The mineral composition of cacauí seed powder reinforces the nutritional potential of Amazonian *Theobroma* species as sources of essential elements relevant to human health and food applications. Similar mineral distributions have been reported in cocoa and cupuaçu seeds, highlighting the technological and nutritional value of these varieties [12].

4 Conclusions

Ultrasound pre-treatment effectively modified the structural, chemical, thermal, and functional properties of *Theobroma speciosum* (cacauí) seed powder without causing significant chemical degradation. FTIR analysis confirmed the preservation of the main functional groups, while SEM micrographs revealed increased porosity, particle fragmentation, and cell wall disruption, facilitating the release of intracellular bioactive compounds. The identification of theacrine further highlights the potential of cacauí as a valuable source of nutraceutical alkaloids with stimulant and antioxidant properties. Thermogravimetric analysis demonstrated that ultrasound treatment preserved the thermal stability of the material, supporting its suitability for subsequent industrial processing. Among the evaluated conditions, the treatment performed at 70% amplitude for 12 min (C70/12) provided the highest total phenolic content and antioxidant activity, indicating that acoustic cavitation enhanced the availability of bioactive metabolites. However, mineral concentrations varied according to the specific combination of ultrasound amplitude and processing time, showing that the condition that maximized bioactive compound recovery did not simultaneously maximize mineral retention. Nevertheless, the qualitative mineral profile and the predominance of the main macro- and microminerals were maintained. Together with the favorable proximate composition, these findings reinforce the nutritional and functional potential of cacauí seed powder as a source of lipids, proteins, minerals, and bioactive compounds. These findings demonstrate that ultrasound represents an efficient, environmentally friendly, and scalable pre-treatment technology for improving the functional quality of Amazonian plant materials. The enhanced availability of bioactive compounds broadens the potential application of cacauí seed powder as a functional ingredient in foods, dietary supplements, nutraceutical formulations, and pharmaceutical and biotechnological products, contributing to the sustainable valorization of underutilized Amazonian biodiversity. Future studies should focus on optimizing ultrasound processing parameters at industrial scales, evaluating the bioaccessibility and bioavailability of the released bioactive compounds, assessing storage stability and shelf life, and investigating the incorporation of ultrasound-treated cacauí seed powder into functional food formulations. Additionally, further studies on the biological activities of theacrine-rich extracts

and their mechanisms of action may expand the pharmaceutical and nutraceutical applications of this promising Amazonian resource.

Supplementary Information The online version contains supplementary material available at https://doi.org/10.1007/s44187-026-01225-z.

Acknowledgements The authors gratefully acknowledge the financial support provided by the Conselho Nacional de Desenvolvimento Científico e Tecnológico (CNPq) and Coordenação de Aperfeiçoamento de Pessoal de Nível Superior (CAPES) for funding and fellowships. The authors also thank the Fundação de Amparo à Pesquisa do Estado do Amazonas (FAPEAM), through the Support Program for Stricto Sensu Graduate Studies (POSGRAD), for the scholarship granted. The authors acknowledge the Analytical Centers at Instituto Federal do Amazonas – Campus Manaus Centro (IFAM-CMC) and Universidade Federal do Amazonas (UFAM) for providing laboratory infrastructure. Additional analytical support and facilities were provided by the Biomolecule Purification Laboratory of the Multidisciplinary Support Center and the Chemical Analytical Center at UFAM, as well as the Samsung SRBR WTS Laboratory and the Laboratório de Pesquisas e Ensaios de Combustíveis (UFAM). The authors thank the Multiuser Center for the Analysis of Biomedical Phenomena of the Universidade do Estado do Amazonas (CMABio) for the scanning electron microscopy (SEM) analyses. The authors would like to thank Ms. Zaira Malheiros for providing the seed powders of Theobroma speciosum.

Author contributions Conceptualization: JMM and JdeAB; Methodology: JMM, DdeQR, CMR, FJM, DNM and VFK; Investigation: JMM, DdeQR, AdeSC, EOdosS and FdasCdoA; Data Curation: JMM, DdeQR, AdeSC and JdeAB; Writing—original draft preparation: JMM and DdeQR; Writing—review and editing: JMM, JdeAB, EAS, PHC and RFC. Visualization: JdeAB, EAS and PHC.

Funding The authors declare that this work received no financial support from public, private, or non-profit funding agencies.

Data availability The datasets used and/or analysed during the current study are available from the corresponding author on reasonable request.

Declarations

Ethics approval and consent to participate The plant material used in this study consisted of cacauí seeds (*Theobroma speciosum* Willd. ex Spreng), of cultivated origin, obtained at km 14 in the municipality of Careiro Castanho, Amazonas, Brazil. All applicable ethical and legal guidelines were followed, and the study was duly registered in the National System for the Management of Genetic Heritage and Associated Traditional Knowledge (SisGen) under registration number A9F3E4F. As the material was cultivated, no specific authorization or permits for collection from wild populations were required. The botanical identification of the species was carried out by Valdely Ferreira Kinupp. A voucher specimen was deposited in a publicly accessible collection at the Herbarium of the Federal Institute of Education, Science and Technology of Amazonas (EAFM), under voucher number EAFM nº 17.682, ensuring traceability and access to the material for future reference.

Consent for publication Not applicable.

Competing interests The authors declare no competing interests.

Open Access This article is licensed under a Creative Commons Attribution-NonCommercial-NoDerivatives 4.0 International License, which permits any non-commercial use, sharing, distribution and reproduction in any medium or format, as long as you give appropriate credit to the original author(s) and the source, provide a link to the Creative Commons licence, and indicate if you modified the licensed material. You do not have permission under this licence to share adapted material derived from this article or parts of it. The images or other third party material in this article are included in the article's Creative Commons licence, unless indicated otherwise in a credit line to the material. If material is not included in the article's Creative Commons licence and your intended use is not permitted by statutory regulation or exceeds the permitted use, you will need to obtain permission directly from the copyright holder. To view a copy of this licence, visit http://creativecommons.org/licenses/by-nc-nd/4.0/.

References

1. Akther S, Akhtaruzzaman M, Islam MR, Ahmed T, Ahmed S, Biswas M. Impact of ultrasound-assisted mild heat treatment on safety, quality, and shelf life of fresh watermelon juice. Food Chem Adv. 2026;10:101222. https://doi.org/10.1016/j.focha.2026.101222.
2. Acik G, Utebay DZ. Ultrasound enhances phenolic and mineral extraction from lemon-chokeberry functional juice. J Food Meas Charact. 2026;20:10997–1009. https://doi.org/10.1007/s11694-026-04386-8.
3. Benítez V, Rebollo-Hernanz M, Braojos C, Cañas S, Gil-Ramírez A, Aguilera Y, Martín-Cabrejas MA. Changes in the cocoa shell dietary fiber and phenolic compounds after extrusion determine its functional and physiological properties. Curr Res Food Sci. 2023;6:1–12. https://doi.org/10.1016/j.crfs.2023.100516.
4. Bento NA, Crispim M, dos Santos Lima A, Silva TC, da Silva Cruz L, da Silva GKP, Ionta M, Ferreira-Silva GÁ, dos Anjos Cruz JM, de Queiroz Rocha D, de Araújo Bezerra J, Azevedo L. Bioprospecting of the Amazonian mapati fruit (Pourouma cecropiifolia Martius): antiproliferative and antimalarial potential of peel and seed hydroethanolic extracts. Food Res Int. 2026;228:118297. https://doi.org/10.1016/j.foodres.2025.118297.
5. Cerri M, Reale L, Zadra C. Metabolite Storage in *Theobroma cacao* L. Seed: cyto-histological and phytochemical analyses. Front Plant Sci. 2019;10:1–11. https://doi.org/10.3389/fpls.2019.01599.
6. Chemat F, Rombaut N, Sicaire AG, Meullemiestre A, Fabiano-Tixier AS, Abert-Vian M. Ultrasound assisted extraction of food and natural products. Mechanisms, techniques, combinations, protocols and applications. Rev Ultrason Sonochemistry. 2017;34:540–60. https://doi.org/10.1016/j.ultsonch.2016.06.035.
7. Collazos-Escobar GA, Barrios-Rodríguez YF, Bahamón-Monje AF, Gutiérrez-Guzmán N. Mid-infrared spectroscopy and machine learning as a complementary tool for sensory quality assessment of roasted cocoa-based products. Infrared Phys Technol. 2024;141:1–10. https://doi.org/10.1016/j.infrared.2024.105482.
8. de Araujo QR, Baligar VC, Loureiro GAHA, de Souza Júnior JO, Comerford NB. Impact of soils and cropping systems on mineral composition of dry cacao beans. J Soil Sci Plant Nutr. 2017;17:410–28. https://doi.org/10.4067/S0718-95162017005000030.
9. Dzah CS, Duan Y, Zhang H, Wen C, Zhang J, Chen G, Ma H. The effects of ultrasound assisted extraction on yield, antioxidant, anticancer and antimicrobial activity of polyphenol extracts: a review. Food Bioscience. 2020;35:100547. https://doi.org/10.1016/j.fbio.2020.100547.
10. Fonseca Júnior EQda, de Queiroz Rocha D, Souza Coelho Oliveira E, Oliveira da Silva S, Amaral Souza FdasCdo, Furlaneto G, da Silva Cruz L, Azevedo L, Frota, Corrêa R, Aparecido Sanches E, Campelo PH, de Araújo Bezerra J. Chemical characterization, nutritional profile, and cytotoxicity potential of Amazonian Theobroma sylvestre Mart. fruits. Food Bioscience. 2025;73:107673. https://doi.org/10.1016/j.fbio.2025.107673.
11. Gangil S. Dominant thermogravimetric signatures of lignin in cashew shell as compared to cashew shell cake. Bioresour Technol. 2014;155:15–20. https://doi.org/10.1016/j.biortech.2013.12.087.
12. Gattward JN, Almeida AAF, Souza JO, Gomes FP, Kronzucker HJ. Sodium-potassium synergism in *Theobroma cacao*: stimulation of photosynthesis, water-use efficiency and mineral nutrition. Physiol Plant. 2012;146:350–62. https://doi.org/10.1111/j.1399-3054.2012.01621.x.
13. González-Silva N, Nolasco-González Y, Aguilar-Hernández G, Sáyago-Ayerdi SG, Villagrán Z, Acosta JL, Montalvo-González E, Anaya-Esparza LM. Ultrasound-assisted extraction of phenolic compounds from *Psidium cattleianum* leaves: optimization using the response surface methodology. Molecules. 2022;27:1–16. https://doi.org/10.3390/molecules27113557.
14. Jean-Marie E, Jiang W, Bereau D, Robinson JC. *Theobroma cacao* and *Theobroma grandiflorum*: botany, composition and pharmacological activities of pods and seeds. Foods. 2022;11:1–23. https://doi.org/10.3390/foods11243966.
15. Khadhraoui B, Turk M, Fabiano-Tixier AS, Petitcolas E, Robinet P, Imbert R, Maâtaoui ME, Chemat F. Histo-cytochemistry and scanning electron microscopy for studying spatial and temporal extraction of metabolites induced by ultrasound. Ultrason Sonochem. 2018;42:482–92. https://doi.org/10.1016/j.ultsonch.2017.11.029.
16. Küçükduman Y, Korkmaz İD, Çiftçi HG, Argün S, Bilge Özel G, Taştan Ülkü Ö, Toker ÖS, Mutlu Z. Monitoring of cocoa quality and conching, tempering, cooling processes in chocolate production with FTIR spectroscopy. J Food Meas Charact. 2026;20:1–12. https://doi.org/10.1007/s11694-025-03986-0.
17. Kumar K, Srivastav S, Singh V. Ultrasound assisted extraction (UAE) of bioactive compounds from fruit and vegetable processing by-products: a review. Ultrason - Sonochemistry. 2021;70:105325. https://doi.org/10.1016/j.ultsonch.2020.105325.
18. Lewis C, Lennon AM, Eudoxie G, Sivapatham P, Umaharan P. Plant metal concentrations in *Theobroma cacao* as affected by soil metal availability in different soil types. Chemosphere. 2021;262:127749. https://doi.org/10.1016/j.chemosphere.2020.127749.
19. Levent O, Şimşek MA, Yıkmış S, Demirel S, Demirok NT, Türkol M, Aljobair MO, Tokatlı N, Ahmed M, I. A. Ultrasound-assisted sustainable processing of garden cress juice: enhancing bioactive compounds and bioaccessibility through XGBoost optimization. ACS Omega. 2025;10:59300–13. https://doi.org/10.1021/acsomega.5c08691.

20. Londoño-Larrea P, Villamarin-Barriga E, García AN, Marcilla A. Study of cocoa pod husks thermal decomposition. Appl Sci (Switzerland). 2022;12:15. https://doi.org/10.3390/app12189318.
21. Mar JM, Carolino AS, Neves KOG, Corrêa RF, Machado MB, Rocha, Dde Q, Kinupp VF, Sanches EA, Campelo PH, Bezerra JA. Enhancing the extraction efficiency of beneficial compounds from *Tapirira guianensis* fruit using ultrasound-assisted extraction and choline chloride deep eutectic solvent. Food Sci Technol. 2025;45:1–8. https://doi.org/10.5327/fst.493.
22. Mar JM, da Fonseca Júnior EQ, Corrêa RF, Campelo PH, Sanches EA, Bezerra JA. Theobroma spp.: a review of it's chemical and innovation potential for the food industry. Food Chem Adv. 2024;4:1–17. https://doi.org/10.1016/j.focha.2024.100683.
23. Mar JM, Frota R, Ramos S, Kinupp VF, Sanches EA, Campelo PH, Bezerra JA. Enhancing Bioactive compound bioaccessibility in *Tapirira guianensis* juices through ultrasound-assisted applications. Process. 2023;11:1–16. https://doi.org/10.3390/pr11092718.
24. Mar JM, Souza L, Picanço W, Bezerra A. Edible flowers from T*heobroma speciosum*: aqueous extract rich in antioxidant compounds. Food Chem. 2021;356:129723. https://doi.org/10.1016/j.foodchem.2021.129723.
25. Millena CG, Balonzo ARR, Rentoy JR, Ruivivar SS, Bobiles SC. Effect of fermentation stages on the nutritional and mineral bioavailability of cacao beans (*Theobroma cacao* L). J Food Compos Anal. 2023;115:104886. https://doi.org/10.1016/j.jfca.2022.104886.
26. Ogunlaja OO, Moodley R, Baijnath H, Jonnalagadda SB. Elemental distribution and health risk assessment of the edible fruits of two ficus species, *Ficus sycomorus* L. and *Ficus burtt-davyi* Hutch. Biol Trace Elem Res. 2020;198:303–14. https://doi.org/10.1007/s12011-020-02048-4.
27. Oracz J, Zyzelewicz D. In vitro antioxidant activity and ftir characterization of high-molecular weight melanoidin fractions from different types of cocoa beans. Antioxidants. 2019;8:1–16. https://doi.org/10.3390/antiox8110560.
28. Orizano-Ponce E, Santillan G, Chamorro-Gómez RE, Villanueva-Tiburcio JE, Estacio-Laguna R, Cueto-Rosales CR, Palma-Lozano D, Cámara F, Cano D. Effect of ultrasound on the physical, morphological, and mechanical properties of bioplastic obtained from lucuma seed starch (*Pouteria lucuma*). Appl Food Res. 2025;5:1–11. https://doi.org/10.1016/j.afres.2025.100990.
29. Osei PA, Kpodo FM, Tettey CO, Dzah CS, Agbenorhevi JK, Hunkpe G, Nanga S. Proximate composition, phenolic, and antioxidant properties of soursop fruit parts. CYTA - J Food. 2023;21:475–80. https://doi.org/10.1080/19476337.2023.2227250.
30. Palmeira L, Pereira C, Dias MI, Abreu RMV, Corrêa RCG, Pires TCSP, Alves MJ, Barros L, Ferreira ICFR. Nutritional, chemical and bioactive profiles of different parts of a Portuguese common fig (*Ficus carica* L.) variety. Food Res Int. 2019;126:108572. https://doi.org/10.1016/j.foodres.2019.108572.
31. Panda D, Manickam S. Cavitation technology-the future of greener extraction method: a review on the extraction of natural products and process intensification mechanism and perspectives. Appl Sci (Switzerland). 2019;9:1–21. https://doi.org/10.3390/app9040766.
32. Ponce J, María S, Zurita G, Peñuela MC. Reproductive ecology of white cacao (*Theobroma bicolor* Humb. & Bonpl.) in Ecuador, western Amazonia: floral visitors and the impact of fungus and mistletoe on fruit production. Brazilian J Bot. 2021;44:479–89. https://doi.org/10.1007/s40415-021-00709-9.
33. Prempeh NYA, Nunekpeku X, Murugesan A, Li H. Ultrasound in the Food Industry: mechanisms and Applications for Non-Invasive Texture and Quality Analysis. Foods. 2025;14:1–16. . https://doi.org/10.3390/foods14122057
34. Rajewska K, Mierzwa D. Influence of ultrasound on the microstructure of plant tissue. Innovative Food Sci Emerg Technol. 2017;43:117–29. https://doi.org/10.1016/j.ifset.2017.07.034.
35. Rojas M, Ruano D, Orrego-Restrepo E, Chejne F. Non-isothermal kinetics of cellulose, hemicellulose, and lignin degradation during cocoa bean shell pyrolysis. Biomass Bioenergy. 2023;177:106932. https://doi.org/10.1016/j.biombioe.2023.106932.
36. Santos IA, Conceição DG, Viana MB, Silva GJ, Santos LS, Ferrão SPB. NIR and MIR spectroscopy for quick detection of the adulteration of cocoa content in chocolates. Food Chem. 2021;349:1–6. https://doi.org/10.1016/j.foodchem.2021.129095.
37. Santos NC, Almeida RLJ, Albuquerque JC, de Andrade EWV, Gregório MG, Santos RMS, Rodrigues TJA, Carvalho RO, Gomes MMA, Moura HV, de Figueiredo DVP, Araújo MA, Lima, VRdo N, Mota MMA. Optimization of ultrasound pre-treatment and the effect of different drying techniques on antioxidant capacity, bioaccessibility, structural and thermal properties of purple cabbage. Chem Eng Process - Process Intensif. 2024;201:1–12. https://doi.org/10.1016/j.cep.2024.109801.
38. Shahidi F, Ambigaipalan P. Phenolics and polyphenolics in foods, beverages and spices: antioxidant activity and health effects—a review. J Funct Foods. 2015;18:820–97. https://doi.org/10.1016/j.jff.2015.06.018.
39. Shen L, Pang S, Zhong M, Sun Y, Qayum A, Liu Y, Rashid A, Xu B, Liang Q, Ma H, Ren X. A comprehensive review of ultrasonic assisted extraction (UAE) for bioactive components: principles, advantages, equipment, and combined technologies. Ultrason Sonochem. 2023;101:106646. https://doi.org/10.1016/j.ultsonch.2023.106646.

40. Soares TF, Oliveira MBPP. Cocoa By-Products: characterization of Bioactive Compounds and Beneficial Health Effects. Molecules. 2022;27:1–23. https://doi.org/10.3390/molecules27051625.
41. Sun Y, Liu Z, Wang J. Ultrasound-assisted extraction of five isoflavones from *Iris tectorum* Maxim. Sep Purif Technol. 2011;78:49–54. https://doi.org/10.1016/j.seppur.2011.01.017.
42. Türkol M, Yıkmış S, Tokatlı N, Sağcan N, Khalid W, Yinanç A, Aksu H, Althawab SA, Alsulami T, Ahmed M, I. A. Ultrasound technology in environmental sustainability: vinegar production from black carrot pulp. Ital J Food Sci. 2026;38(1):153–67. https://doi.org/10.15586/ijfs.v38i1.2944.
43. Umaña M, Calahorro M, Eim V, Rosselló C, Simal S. Measurement of microstructural changes promoted by ultrasound application on plant materials with different porosity. Ultrason Sonochem. 2022;88:106087. https://doi.org/10.1016/j.ultsonch.2022.106087.
44. Vardanega R, Santos DT, De Almeida MA. Intensification of bioactive compounds extraction from medicinal plants using ultrasonic irradiation. Pharmacogn Rev. 2014;8:88–95. https://doi.org/10.4103/0973-7847.134231.
45. Vilkhu K, Mawson R, Simons L, Bates D. Applications and opportunities for ultrasound assisted extraction in the food industry—a review. Innovative Food Sci Emerg Technol. 2008;9:161–9. https://doi.org/10.1016/j.ifset.2007.04.014.
46. Yusoff IM, Mat Taher Z, Rahmat Z, Chua LS. A review of ultrasound-assisted extraction for plant bioactive compounds: phenolics, flavonoids, thymols, saponins and proteins. Food Res Int. 2022;157:111268. https://doi.org/10.1016/j.foodres.2022.111268.
47. Zabot GL, Viganó J, Silva EK. Low-frequency ultrasound coupled with high-pressure technologies: impact of hybridized techniques on the recovery of phytochemical compounds. Molecules. 2021;26:1–20. https://doi.org/10.3390/molecules26175117.

Publisher's note Springer Nature remains neutral with regard to jurisdictional claims in published maps and institutional affiliations.

Authors and Affiliations

Josiana Moreira Mar[1,4] · Daniel de Queiroz Rocha[1,4] · Adriano de Souza Carolino[2] · Camila Macena Ruzo[2] · Daniel Nascimento Motta[1] · Florência João Macamo[3] · Erickson Oliveira dos Santos[5] · Francisca das Chagas do Amaral Souza[6] · Valdely Ferreira Kinupp[7] · Renilto Frota Correa[4] · Edgar Aparecido Sanches[2] · Pedro Henrique Campelo[8] · Jaqueline de Araújo Bezerra[1,9]

✉ Josiana Moreira Mar
josimoreira@ufam.edu.br

✉ Jaqueline de Araújo Bezerra
jaqueline.bezerra@inpa.gov.br

[1] Posgraduate Program in Biotechnology, Federal University of Amazonas, Manaus 69067-005, Brazil

[2] Laboratory of Nanostructured Polymers, Materials Physics Department, Federal University of Amazonas, Manaus 69067-005, Brazil

[3] LAPEC, Fuel Research and Testing Laboratory, Federal University of Amazonas, Manaus 69067-005, Brazil

[4] NECTAM, Analytical Center, Federal Institute of Education, Science and Technology of Amazonas, Campus Manaus Centro, Manaus 69020-120, Brazil

[5] Research Laboratory for Water Reuse, Samsung Research & Development Institute Brazil, Samsung Eletrônica da Amazônia, Manaus 69075-842, Brazil

[6] Laboratory of Physical Chemistry of Food (LFQA), National Amazon Research Institute (INPA), Manaus 69055-010, Brazil

[7] Federal Institute of Education Science and Technology of Amazonas (IFAM), Manaus, AM, Brazil

[8] Department of Food Technology, Federal University of Viçosa, Viçosa 36570-900, Brazil

[9] Coordination of Technology and Innovation (COTEI), National Institute for Amazonian Research (INPA), Manaus, Amazonas, Brazil